

A Novel Dual-band Small Size Microstrip Antenna

Abdel Fattah Sheta¹, Hoda Boghdady², Ashraf Mohra³
and Samir F. Mahmoud⁴

^{1,3} EE Dept. King Saud University, P. O.Box 800, Riyadh 11421, Saudi Arabia

² Transmission Dept., NTI, 11768, Cairo, Egypt

⁴ EE Dept., Kuwait University, P. O.Box 5969, Safat 13060, Kuwait

Abstract – A new small size dual-band microstrip antenna structure is proposed. The antenna consists of two resonant elements designed separately and integrated in such a manner to improve the compactness of the dual band structure and maintain the performance of each element. The structure is analyzed using lumped element approach and design curves are produced. The proposed approach is validated through a design example using theoretical curves and simulations. Implementation of an antenna operating in the 900 MHz and 1800 MHz bands is presented and comparisons between simulated and experimental results are given.

I. INTRODUCTION

In many regions over the world the two operating frequency systems, GSM system operating at 900 MHz, and the DCS 1800 at 1800 MHz, are simultaneously used for mobile communications. Therefore, the design of dual-band antennas for mobile handset applications has received much attention. Beside its dual-band operation, the antenna should also be small in size and excited by a single feed to meet the handset requirements. Due to their inherent flexibility, planar antennas are the most appropriate candidates to achieve these requirements. Recently, various types of planar inverted-F antennas (PIFAs) have been proposed for such applications [1]-[7]. Most of the previous works were based on simulator packages that use finite-difference time-domain (FDTD) or the method of moment. In this case the selection of the antenna dimensions for dual band operation becomes a tedious job.

In this paper, we propose a compact, dual band microstrip antenna that consists of two resonant elements. Each element can be designed separately at a specified center frequency and both elements integrated in such a way to maintain matching at the two frequencies, to have a compact structure and to provide negligible effect on each other. Each element consists of a short-circuited narrow line connected to a wider open circuited line as shown in Fig. 1. The lower frequency element (Fig. 1a) is a T-shaped patch and the high frequency element is an L-shaped patch (Fig. 1b). Both elements have a short circuited pin at the end of the narrow arm. The integrated dual band antenna is shown in Fig. 1c. The lumped

element model extracted from the transmission line theory is used to predict the resonant frequency of each element. The lumped element equivalence of the antenna elements is described in the next section where design curves are introduced. Discontinuities effects are explained in Section 3. In Section 4, we introduce specific design cases and conclusions are given in Section 5.

II. LUMPED ELEMENT EQUIVALENCE OF THE PROPOSED ANTENNA ELEMENTS

The simplest microstrip resonator is a half wavelength line opened at both ends, or a quarter wavelength line opened at one end and short-circuited at the other. Unfortunately, the size of an antenna based even on a quarter wavelength line is physically too large to be used for handset GSM applications. For this reason, a shaped short circuit resonator such as short circuited H-structure [8] or T-structure [9], which is considered as half of an open H-shaped antenna [10], has been developed as a compact antenna for single frequency operation. The H-shaped antenna has been analyzed using FDTD method, while the T-shaped one has been analyzed using the magnetic wall concept and transmission line theory.

The proposed dual-band antenna is shown in Fig. 1c and consists of two elements: a T-element that resonates at the lower frequency (Fig. 1a) and an L-element that resonates at the higher frequency (Fig. 1b). The transmission line equivalence of the short-circuited resonator elements in Figs. 1a and 1b are shown in Figs. 2a and 2b, respectively. For the T-shaped element, θ_1 and θ_2 are the effective electrical lengths of the lines of physical lengths l_1 and l_2 , respectively, after including the discontinuity effects. Z_1 and Z_2 are the characteristic impedances of the microstrip lines of widths W_1 and W_2 , respectively. These transmission lines can be represented by the lumped elements L and C as shown in Fig. 2c. For the T-shaped element (Fig. 1a) the short circuited line is equivalent to a lumped inductance given by:

$$\omega L = Z_1 \tan \theta_1 \quad (1)$$

where $\theta_1 = \omega l_1 / v_{ph1}$, v_{ph1} and Z_1 are the phase velocity and characteristic impedance of a microstrip line of width W_1 and effective length l_1 . The capacitance of the two parallel

open lines is related to their physical dimensions by

$$\omega C = 2 Y_2 \tan \theta_2 \tag{2}$$

where $\theta_2 = \omega l_2 / v_{ph2}$, v_{ph2} and Y_2 are the phase velocity and characteristic admittance ($1/Z_2$) of a microstrip line of width W_2 and effective length l_2 . Now combining (1) and (2) at the resonant frequency $\omega = \omega_0 = 1/\sqrt{LC}$, we get

$$2 \tan \theta_1 \tan \theta_2 = K \tag{3}$$

where K is the ratio of the line impedances; $K = Z_2 / Z_1$. Using (3), θ_2 is plotted against θ_1 for different values of K in Fig. 3a. It is observed that for a given value of θ_1 , θ_2 decreases with decrease of K resulting in a reduction of the total antenna size.

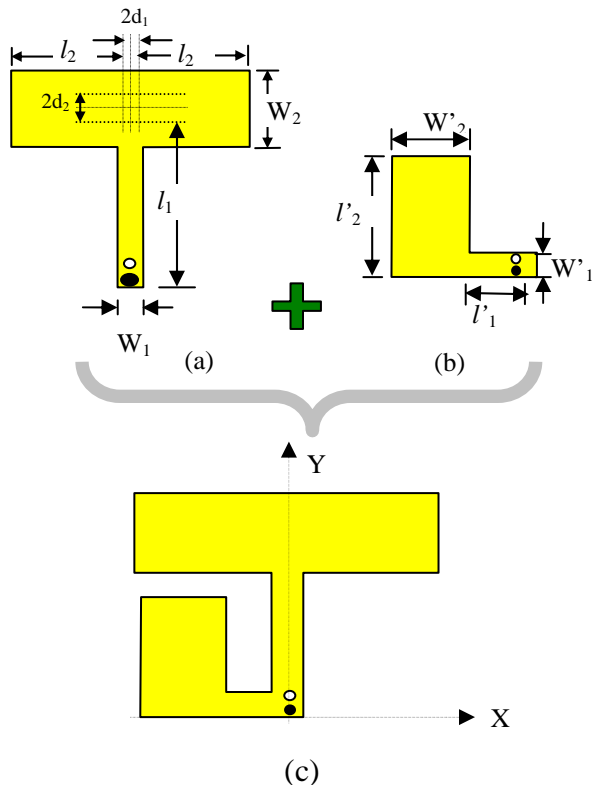


Fig. 1. a) T-shaped antenna operates at the lower frequency, b) L-shaped antenna operates at the higher frequency, and c) Geometry of the proposed dual band antenna.

Similar analysis can be carried out for the L-shaped element. So let us denote by θ'_1 and θ'_2 the effective electrical lengths of the lines l'_1 and l'_2 , respectively. Z'_1 and Z'_2 are the characteristic impedances of the microstrip lines of widths W'_1 and W'_2 , respectively. Following the same steps as for the T-shaped element, at resonance we get:

$$\tan \theta'_1 \tan \theta'_2 = K \tag{4}$$

In this case K is equal to Z'_2/Z'_1 . The design curves for this antenna are drawn in Fig. 3b for the same values of K as in Fig. 3a.

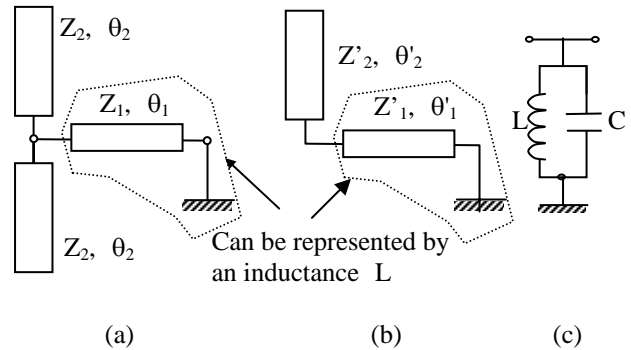


Fig. 2. a) Transmission line equivalence of antenna of Fig. 1a, b) Transmission line equivalence of antenna of Fig. 1b, and c) Lumped element equivalence of the resonators in Fig. 2(a) or 2(b).

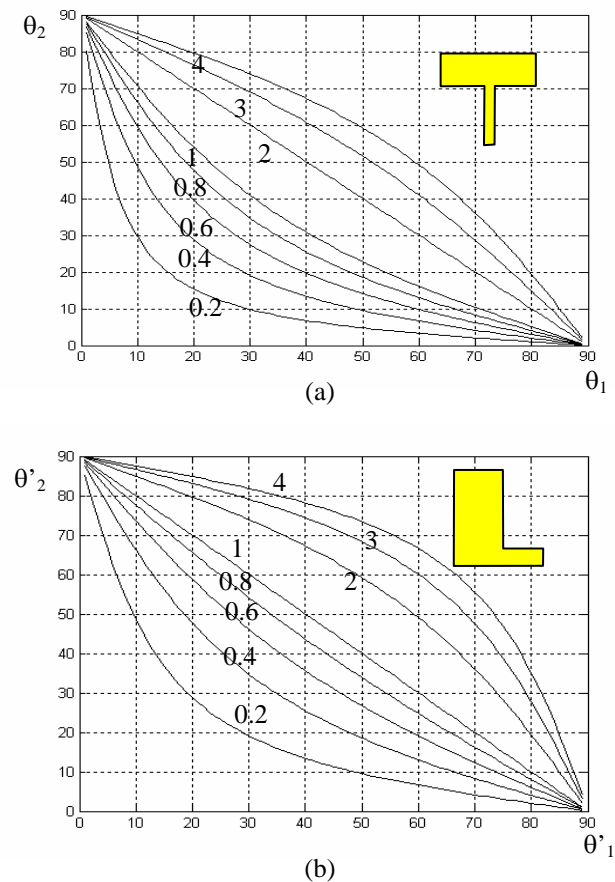


Fig. 3. θ_1 versus θ_2 for different values of K . a) T-shaped antenna, and b) L-Shaped antenna.

In this case the total electrical length of the antenna is given by $\theta'_t = \theta'_1 + \theta'_2$. It is noted that for $K = 1$ (uniform resonator), the total electrical length is 90° while the total length decreases as K decreases.

Figs. 3a and 3b, which determine the electrical lengths of the antenna arms, are helpful for a primary design of the T and L shaped elements through judicious selection of the K factors. The antenna physical dimensions l_1 , l_2 , W_1 , and W_2 (primed and unprimed) can then be calculated for specific frequencies of operation as will be described in the next section.

III. CIRCUIT LAYOUT

The circuit layout shown in Fig. 1, is the result of the conversion of the design parameters Z_1 , θ_1 , Z_2 , θ_2 , Z'_1 , θ'_1 , Z'_2 , and θ'_2 , to a physical dimensions W_1 , l_1 , W_2 , l_2 , W'_1 , l'_1 , W'_2 , and l'_2 in a selected substrate material at a design frequency. However, for wide bandwidth requirements, microstrip antennas are usually implemented on a thick air substrate. In this case, the required discontinuities in the structure significantly affect the resonance frequency of the antenna. Microstrip discontinuity can be represented as an equivalent circuit at some point in the transmission line. The component values, of the equivalent circuit, depend on the parameter of the line and the discontinuity as well as the frequency of operation. In some cases the equivalent circuit involves a shift in the phase reference planes on the transmission lines [11]. One approach for eliminating the discontinuity effect is to construct an equivalent circuit, including it in the design of the circuit, and compensating for its effect by adjusting other circuit parameters. In our case, the effects will be compensated in the lengths of the lines using either closed form expressions or through the aid of the IE3D simulator. The main discontinuities that exist in the proposed structure are the open end, T-junction, shorting post, and the bend.

Open end

An empirical expression for the open-end effect is given in [12, Eq. 1]. It can be used to calculate the equivalent additional line length Δl_{oc} .

Tee junction

The more useful representation of the Tee junction, for the design procedure, is to define the shift in reference planes as shown in Fig. 1a. The reference planes parameters d_1 , and d_2 can be calculated in terms of the substrate parameters and the lines widths W_1 , and W_2 from semi-empirical expressions given in [13, p. 245].

Shorting post

The shorting post is usually characterized by its equivalent inductance. This definition is not suitable to be incorporated in microstrip antenna design since the

resonance frequency is highly dependent of the location of the post. For this reason the shorting post is studied and compensated using the IE3D simulator. This can be achieved, first, by calculating the phase angle of S_{11} of a short circuit line of characteristic impedance Z_1 and electrical length θ_1 from

$$\text{Ang}(S_{11})\Big|_{sc} = 180 - 2 \tan^{-1}\left(\frac{Z_1 \tan \theta_1}{50}\right). \quad (5)$$

After that, an equivalent line of width W and length l terminated by a shorting post can easily be calculated with the optimization procedure tool of the IE3D. The optimization objective in this case is to match the theoretical angle from Eq. (5) to the angle of S_{11} of the physical length l at the design frequency.

Bend

The bend is usually modeled in terms of its equivalent circuit [11], which is not easy to compensate for in the lines lengths. However, it is easy to compensate for the bend and the open end, simultaneously, of the L-shape through the optimization tool of the IE3D. This can easily be performed by equating the phase angle of S_{11} of the open circuit layout in Fig. 4c to the theoretical angle of the open circuited line given by

$$\text{Ang}(S_{11})\Big|_{oc} = -180 + 2 \tan^{-1}\left(\frac{Z'_2 \cot \theta'_2}{50}\right). \quad (6)$$

For thin conventional dielectric materials, where, $2 < \epsilon_r < 10$ and thickness $0.5 < h < 2$ mm, the use of closed form expressions [11-13] for most of the microstrip discontinuities below 10 GHz leads to very good results.

IV. DESIGN CASE

The design approach described in the previous section is now validated through the design of an antenna that operates in the 900/1800 MHz bands. An air substrate of thickness 6.4 mm is used. Considering the T-shaped element, the thin line width W_1 is selected to be 2 mm. This small value helps to reduce any parasitic loading between the T and L elements after their integration. The resultant characteristic impedance of this line is $Z_1 = 193 \Omega$. Now, if we take the impedance ratio $K = 0.6$, the characteristic impedance of the wide line, Z_2 will be 115.8Ω , corresponding to about 7.7 mm line width W_2 . Fig. 3a is now used to compromise between θ_1 and θ_2 . Taking $\theta_1 = 25^\circ$, θ_2 is 32.8° . A probe feed of radius 0.5 mm is located close to the shorting post of radius 0.3 mm. For ideal lines with no discontinuity effects, the physical lengths of this element calculated at 900 MHz correspond to 25° and 32.8° would be 23.2 mm and 30.4 mm,

respectively. The physical dimensions shown in Fig. 1a are calculated as follows:

$$\Delta l_{oc} = 3.1 \text{ mm [12, Eq. 1].}$$

d_1 and d_2 are computed as 0.4 mm and 3.2 mm, respectively by use of [13, p. 245], while $l_2 = 30.4 - 3.1 = 27.3$ mm.

l_1 is obtained from the IE3D to match the theoretical phase angle of S_{11} , calculated from Eq. (5) as 58.1° , to the angle of the line terminated by a shorting post of radius 0.3 mm located as shown in Fig. 4a. The optimum length for l_1 is 19.4 mm. This means that, the effect of the shorting post at this position is equivalent to a line of the same width 2 mm and 3.8 mm length at 900 MHz.

The simulated resonance frequency corresponding to these dimensions is 935 MHz. This little variation is due to the neglect of feeder effect and the accuracy of the model used to calculate the reference planes. Slight increase of l_1 to 19.7 mm and l_2 to 28.6 mm reduces the resonance frequency to 908 MHz. In order to do a further reduction of the area occupied, the right arm of the T element is bent parallel to the narrow arm as shown in the inset of Fig. 5a. The effect of the bend is accounted for by using the simulator, and the simulation results of $|S_{11}|$ are given in Fig. 5a. The resonant frequency of the T-shaped element is 908 MHz and the bandwidth, corresponding to a 10 dB return loss, is 8 MHz.

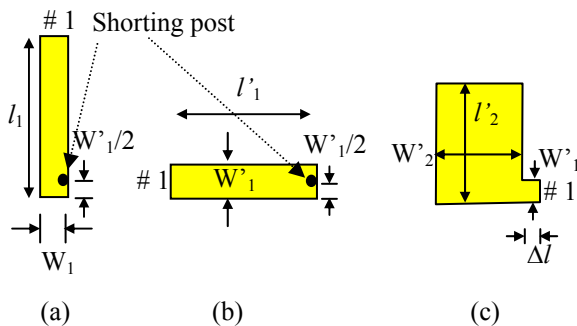
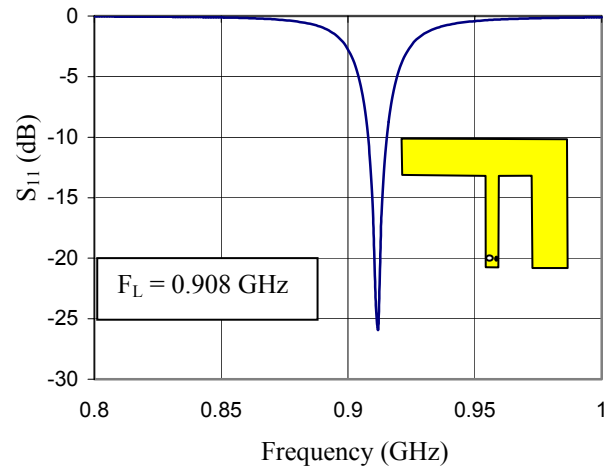


Fig. 4. Circuit layout elements to calculate discontinuities effect (a) the shoring post for the T-shaped at 900 MHz, (b) the shoring post of the L-shaped at 1800 MHz, and (c) the bend and open circuit effect of the L-shaped at 1800 MHz.

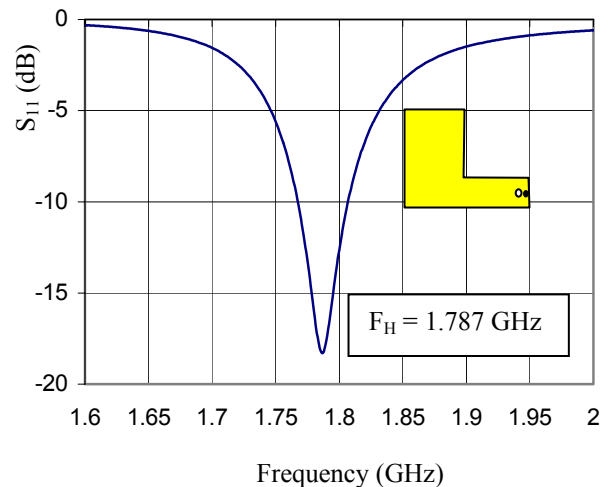
Similar steps are used to design the L-shaped antenna element at 1800 MHz. The narrower line width is selected to be $W'_1 = 3$ mm which corresponds to a characteristic impedance of 169Ω . Taking the impedance ratio $K = 0.5$, the characteristic impedance of the wider line is 84.5Ω which requires a line width of 14 mm. Taking $\theta'_1 = 28^\circ$ in Fig. 3b, θ'_2 is 43° . For ideal transmission line elements,

the physical lengths would be 13 mm, and 19.9 mm for narrow and wide lines, respectively. The physical dimensions of the L-shaped circuit layout shown in Fig. 1b are calculated as follow:

The length of the narrow line ended by a shorting post of 0.3 mm radius, shown in Fig. 4b, is calculated by equating the phase angle of S_{11} from the IE3D with the theoretical value from Eq. (5) for Z'_1 and θ'_1 at 1800 MHz. The resultant l'_1 is 6.5 mm. This means that the shorting post at this position is equivalent to a line of 3mm width and 6.5 mm length.



(a)



(b)

Fig. 5. Simulated S_{11} of the separate T and L shaped elements designed on air substrate of 6.4 mm thickness, a) Simulation results of the T-shape element designed at 900 MHz, and b) Simulation results of the L-shape element designed at 1800 MHz.

The bend is then calculated by the help of the optimization procedure of the IE3D as described in the previous section. The theoretical angle of the open circuited line from Eq. (6) is -57.8° . The circuit layout proposed is shown in Fig. 4c. The short length Δl is chosen to be 1.8 mm. The optimum value of the length l_2 to match this angle is 11.5 mm. The simulated resonance frequency obtained based on these dimensions is 1870 MHz. The shift in the resonance frequency is due to the feeder effect. This can be simply modified by little increase in any length of the circuit. For $l_2 = 15.4$ mm the simulated resonance frequency becomes 1787 MHz. The simulation results for the L-shaped element are shown in Fig. 5b where the 10 dB return loss bandwidth is 40 MHz at the center frequency.

Integration of the dual band antenna: Now the two elements are integrated as in Fig. 1c, while maintaining the same shorting post and feeder locations. The simulation results of the integrated structure are shown in Fig. 6. The lower band and upper band resonance occur now at $f_L = 907$ MHz and $f_H = 1835$ MHz with bandwidths of 8 MHz and 24 MHz respectively. It is thus seen that while the integration has almost no effect on the center frequency and bandwidth at the lower band, it caused an increase of the resonant frequency at the higher band by about 48 MHz, and a reduction in the bandwidth from 40 MHz to 24 MHz. We attribute this frequency shift and bandwidth reduction to the parasitic loading of the T- element on the L-element at the higher band. The simulated radiation patterns at the two resonant frequencies are plotted in Figs. 7 and 8. Both show an approximate omnidirectional radiation in the azimuth plane (x-z plane).

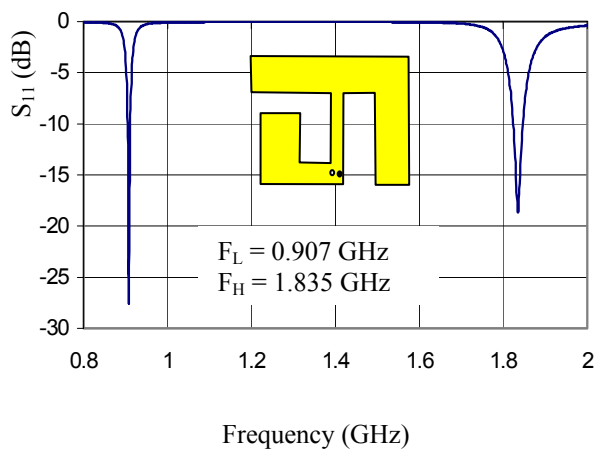


Fig. 6. Simulated S_{11} of the integrated T and L shaped elements in Figs. 5a and 5b.

The antenna gain is computed to be about -0.15 dBi and 1.5 dBi for the lower and upper resonant frequencies, respectively. Such relatively low gains are typical for compact antennas [6], [14]. We note that the antenna efficiency at the lower band is about 70%, so while the gain is -0.15 dBi the antenna directivity is equal to 1.8 dBi.

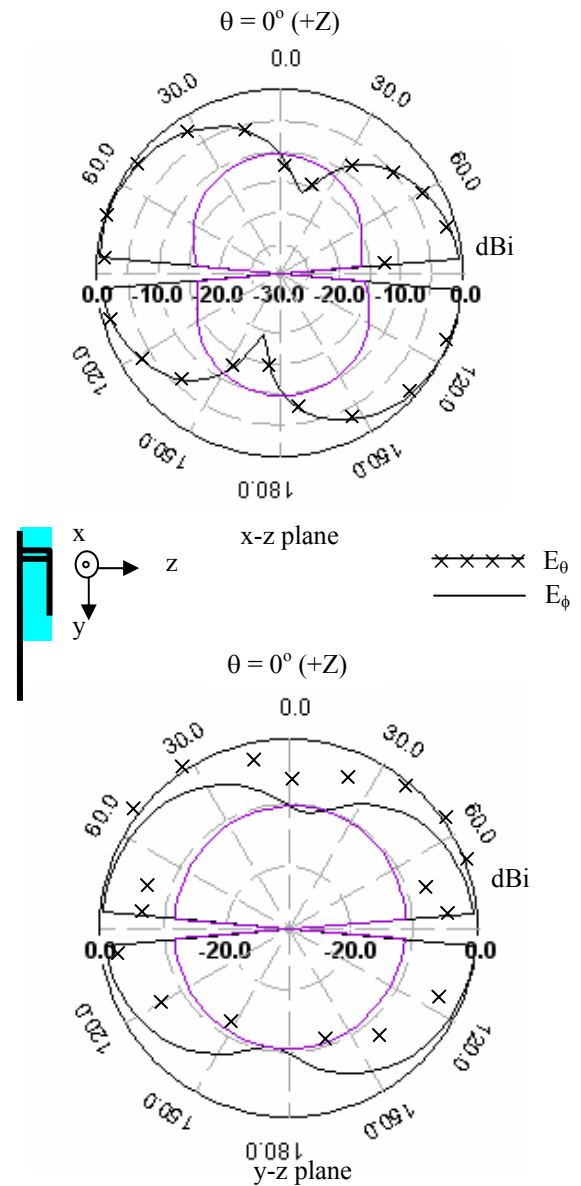


Fig. 7. Simulated radiation patterns at 907 MHz for the antenna in Fig. 5a.

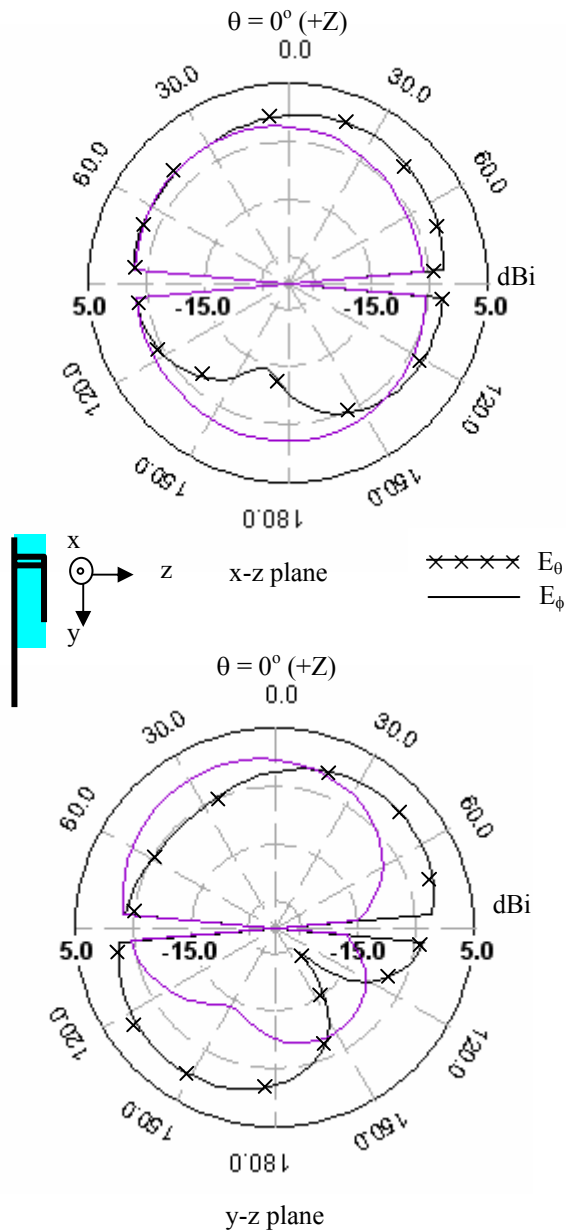


Fig. 8. Simulated radiation patterns at 1835 MHz for the antenna in Fig. 5a.

Experimental work: The dual band antenna is built on a foam substrate with dielectric constant close to that of air. The ground plane used is a copper plate of dimensions $64 \times 47 \text{ mm}^2$. The experimental results are shown in Fig. 9. The measured bandwidths based on 10 dB return loss, are about 12 and 31 MHz (compared to 8 MHz and 24 MHz from simulations) centered at 870 MHz and 1756 MHz, respectively. The observed change of the center frequencies and bandwidths from the simulation results

may be attributed to the inaccurate tools used for installing the feeder and short circuit. Simulations have shown that the resonance frequencies and bandwidths are sensitive to the locations of the short circuit and the feed. In addition, extra losses in the experiment, due to dielectric loss and finite ground plane, may be responsible for the increased experimental bandwidths compared to the simulation results.

Finally, to appreciate the size reduction achieved, we note that the built antenna occupies a volume of $27 \times 44 \times 6.4 \text{ mm}^3$ and mounted on a ground plane of $64 \times 47 \text{ mm}^2$. In terms of the wavelength at 1800 MHz ($\lambda = 166 \text{ mm}$), the antenna volume is about $0.16\lambda \times 0.26\lambda \times 0.04\lambda$ which makes it quite compact.

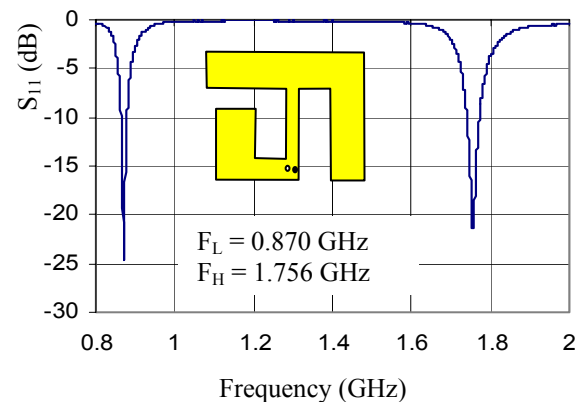


Fig. 9. Measured S_{11} of the integrated T and L shaped elements in Figs. 5a and 5b.

V. CONCLUSION

A new small size dual-band antenna structure has been proposed. Namely a T-patch antenna element tuned at 900 MHz is integrated with an L-patch tuned at 1800 MHz. A simple design procedure based on lumped element representation is used to obtain design equations and curves that are used for a preliminary design. The design is trimmed by using the IE3D simulation tool to account for the end and bend effects. Simulation results show the feasibility of achieving a compact dual band antenna occupying a volume of $0.16\lambda \times 0.26\lambda \times 0.04\lambda$, where λ is the wavelength at the upper band (1800 MHz). The simulation results are validated by building and testing an antenna prototype. Experimental and simulation results show reasonable agreement in terms of the center frequencies and bandwidths.

REFERENCES

- [1] Z. D. Liu, P. S. Hall, and D. Wake, "Dual-frequency planar inverted F antenna," *IEEE Trans. Antennas Propagat.*, vol. 45, pp. 1451–1458, Oct. 1997.
- [2] C. R. Rowell, and R. D. Murch, "A compact PIFA suitable for dual-frequency 900/1800-MHz operation," *IEEE Trans. Antennas Propagat.*, vol. 46, pp. 596–598, April 1998.
- [3] S. Tarvas, and A. Isohatala, "An internal dual-band mobile phone antenna," *Proc. IEEE AP-Symp.*, pp. 266–269, 2000.
- [4] P. Salonen, M. Keskilampi, and M. Kivikoski, "Single-feed dual-band planar inverted-F antenna with U-shaped slot," *IEEE Trans. Antennas Propagat.*, vol. 48, pp. 1262–1267, August 1998.
- [5] G. H. K. Lui, and R. D. Murch, "Compact dual-frequency PIFA designs using LC resonators," *IEEE Trans. Antennas Propagat.*, vol. 49, pp. 1016–1019, July 2001.
- [6] F. R. Hsiao, H. T. Chen, G. Y. Lee, T. W. Chiou, and K. L. Wong, "A dual-band planar inverted-F patch antenna with a branch-line slit," *Microwave Opt. Technol. Lett.*, vol. 32, pp. 310–312, Feb. 2002.
- [7] C. W. Chiu, and F. L. Lin, "Compact dual-band PIFA with multi-resonators," *Electron. Letters*, vol. 38, no. 12, pp. 538–539, 2002.
- [8] D. Singh C. Kallialakis, P. Gardner, and P. S. Hall, "Small H-shaped antennas for MMIC applications," *IEEE Trans. Antennas and Propagat.* vol. 48, pp. 1134–1140, July 2000.
- [9] A. Mohra, A. F. Sheta, and S. F. Mahmoud, "Analysis and design of small size short circuited microstrip T-shaped antenna," *Proc. of 20th National Radio Science Conference*, B18, Cairo, Egypt, 2003.
- [10] A.F. Sheta, A. Mohra, and S. F. Mahmoud, "Multi-band operation of compact H-shaped microstrip patch antenna," *Microwave. Optical Tech. Letters*, vol. 35, pp. 363–367, Dec. 2002.
- [11] B. C. Wadell, *Transmission Line Design Handbook*, Artech House, Norwood, MA, 1991.
- [12] M. R. Kirschning, R. H. Jansen, and N. H. L. Koster, "Accurate model for open end effect of microstrip lines," *Electron Lett.*, Vol. 17, pp. 123–125, 1981.
- [13] T.C. Edwards, and M. B. Steer, *Foundations of Interconnect and Microstrip Design*, John Wiley & Sons, 2000.
- [14] S.F. Mahmoud, and R. K. Deeb, "Characteristics of a circular microstrip patch antenna with a shorting post," *Journal of Electromagnetic Wave Applications*, vol. 16, Feb. 2002.



Abdel fattah sheta received B.S. degree in Communications and Electro - Physics from Alexandria University, Egypt in 1985. He obtained his M.S. degree in Electrical Engineering Department, Cairo University, in 1991. In 1996, he received the Ph.D degree in microwave circuits analysis and design from ENST, Université de Bretagne Occidentale, France. During 1996-1998, he worked as a researcher in the National Telecommunication Institute, Cairo, Egypt. In 1998 he joined Electric Engineering Department, Cairo University, Fayoum Branch. Currently he is an associate Prof. In Electrical Engineering at King Saud University, Saudi Arabia. His current research interests include microstrip antennas, planar and uniplanar MIC's and MMIC's.



Hoda Boghdady graduated from Electronics and Communication Engineering Dept., Cairo University, Egypt in 1983, obtained M.Sc. from Cairo University, Egypt and Ph.D. from North Carolina State University, USA, in 1987 and 1993 respectively. Currently, Deputy Head of the Transmission Dept. at the National Telecommunication Institute in Egypt. Current research interests: microstrip antennas, CAD for planar microwave circuits



Ashraf S. Mohra graduated from the Electronics and Comm. Engineering Dept., Zagazig University, Egypt in 1986. He received the M.Sc. and Ph.D degrees in Electronics and Comm. Department, Ain Shams University, Cairo, Egypt, in 1994 and 2000, respectively. During 1989-2000 he was a researcher in microstrip Department at Electronics Research Institute, Egypt. He worked as a visiting prof., Mansoura University (2000-2002) and Akhbar El-Yom Academy (2003-2005). He was promoted to Associate Prof. in 2005. Currently he works in the Electrical Engineering Department at King Saud University, Saudi Arabia. His current research interests include microstrip antennas, hybrid junctions, computer aided design of planar and uniplanar of MIC's and MMIC's.



Samir F. Mahmoud graduated from the Electronic Engineering Dept., Cairo university, Egypt in 1964. He received the M.Sc and Ph.D. degrees in the Electrical Engineering Department, Queen's university, Kingston, Ontario, Canada in 1970 and 1973. During the academic year 1973-1974, he was a visiting research fellow at the Cooperative Institute for Research in Environmental Sciences (CIRES). Boulder, CO, doing research on Communication in Tunnels. He spent two sabbatical years, 1980-1982, between Queen Mary College, London and the British Aerospace, Stevenage, where he was involved in design of antennas for satellite communication. Currently Dr. Mahmoud is a full professor at the EE Department, Kuwait University. Recently, he has visited several places including Interuniversity Micro-Electronics Centre (IMEC), Leuven, Belgium and spent a sabbatical leave at Queen's University and the royal Military College, Kingston, Ontario, Canada in 2001-2002. His research activities have been in the areas of antennas, geophysics, tunnel communication, e.m wave interaction with composite materials and microwave integrated circuits. He is the author of "Electromagnetic Waveguides; theory and applications", IEE Electromagnetic series, vol. 32. Dr. Mahmoud is a Fellow of IEE and one of the recipients of the best IEEE/MTT paper for 2003.